Sensors & Transducers, Vol. 182, Issue 11, November 2014, pp. 281-287

www.sensorsportal.com

Sensors & Transducers

© 2014 by IFSA Publishing, S. L.
http://www.sensorsportal.com

Finite Element Modeling of Piezoelectric Cantilever with 31 Effects for Sensor Application

[1] Atul, [2] Vinayak Ranjan, [3] Ankit L. Pandey
[1, 2] Indian School of Mines, Dhanbad, 826004, India
[3] University of Florida, Florida, 32611, USA
E-mail: mindmakeupatul@gmail.com, vinayakranjan@gmail.com, ankitpandey@ufl.edu

Received: 5 November 2014 /Accepted: 28 November 2014 /Published: 30 November 2014

Abstract: Energy harvesters that extract energy from vibrating system with the help of piezoelectric cantilever beam show strong potential for powering wireless devices. This paper presents numerical characterization of piezoelectric cantilever beam having rectangular cross-section to enhance the power of energy harvesters. The beam was modeled based upon Euler Bernoulli's beam theory. In this work, piezoelectric cantilever beam with 31 effects was developed to analyze the dynamic behavior of this system with the help of finite element method. It was noticed that the highest tip displacement of cantilever beam was in the second mode at 25 mm length. It was further indicated that second mode of resonant frequency provided higher voltage as compared to first mode of cantilever beam without any proof mass. But when proof mass was added at free end the voltage dropped in the second mode and increased in first mode under a proof mass of 0.40 g. *Copyright © 2014 IFSA Publishing, S. L.*

Keywords: Piezoelectric, Energy harvesting, Finite element modeling.

1. Introduction

Recent developments in the field of sensors have seen to boost in the miniaturization of portable electronic systems. Miniaturization helps to replace batteries by clean and renewable energy sources. Several techniques are used for harvesting energy like electrostatic, electromagnetic and piezoelectric transducers which convert mechanical energy into electrical energy. Out of these three, piezoelectric transducers are the better option to extract maximum energy because of higher electromechanical coupling coefficient. Today piezoelectricity is a matter of great concern receiving a considerable attention due to its high potential applicability for vibration control. Many researchers have done piezoelectric modeling with the help of finite element method for vibration control of active structures [1, 2]. In past decades, wireless sensor came into existence resulting into modeling of energy harvester with the help of piezoelectric cantilever beam for its various applications. Huicong et al. [3] designed a piezoelectric energy harvesting cantilever integrated with silicon proof mass which presents an output voltage of 42 mV at very low resonant frequency of 35.8 Hz. The performance of output voltage with respect to frequency was also demonstrated under the acceleration of 0.1 g. The effects of material properties and geometrical dimensions have great impact upon the performance of energy harvesters which provides useful guidelines for design and modeling. L. Zhou et al. [4] analyzed the combined effects of piezoelectric constitutive equations and single degree of freedom of the shear mode piezoelectric cantilever. They also validated their results with the numerical solutions. Frequencies of

ambient available vibration source are very low and normally range from 20-200 Hz. So in order to extract maximum output voltage the resonant frequency of device has to match the dominant frequency present in the surroundings [4]. Lead Zirconate Titanate, Zinc Oxide, and Aluminum Nitride etc. are demonstrated by various researchers for its actuation capabilities. Cantilever beam with piezoelectric layer plays an important role in improving the harvester's efficiency. Mainly rectangular shaped cantilever beam is used in MEMS Technology as it is easy to fabricate [5]. However, controlling of resonant frequency of piezoelectric energy harvesting device is rarely examined because of the difficulties in the dimensional control of device during fabrication which decides the resonant frequency [6]. It has been reported that the output voltage will be reduced when the driving vibration frequency deviates from the resonant frequency of the device [7]. As size reduces to millimeter scale, it becomes a matter of great issues to fabricate such device with medium resonant frequency because of the specifications of micro fabrication condition, material selection and restriction of device size. Mostly high resonant frequencies MEMS based energy harvesters are reported [8]. Thin film piezoelectric lead zirconate titanate (PZT) materials offer a number of advantages in microelectromechanical systems (MEMS) as such devices provide large motions with low hysteresis in applications such as actuating mirrors [9], and raster scanning mirrors [10]. Hence, PZT thin films are good transducer materials for MEMS based energy harvesters [11]. Vibration-based MEMS energy harvesters have received increasing attention as a potential power source for microelectronics and wireless sensor nodes [12]. Atul and Vinayak reported the numerical investigations of a cantilever having an array of PZT with silicon proof mass. The performance of output voltage with respect to thickness, length and width of PZT patterns was analysed [16].

Present work deals with the finite element modelling of piezoelectric cantilever beam with 31 effects. The beam was modelled with the help of Euler- Bernoulli's beam theory. The performance of output voltage was examined with different proof mass as well as without proof mass. The effect of different lengths of cantilever beam upon tip displacement was also investigated.

2. Generalized Hamilton's Principle for a Piezoelectric Beam for Energy Harvesting

According to Hamilton's principle [13]

$$\int_{t_1}^{t_2}[\,\delta\,(T-U+W_e)+\delta W]dt=0, \qquad (1)$$

where T is the total kinetic energy, U is the total potential energy, We is the electrical energy can be given as

$$T=\int_{V_p}\frac{1}{2}\,\rho_p\,[\dot{\xi}]^t[\dot{\xi}]dV_p \qquad (2)$$

$$U=\int_{V_p}\frac{1}{2}\,[S]^t[\sigma]dV_p \qquad (3)$$

$$W_e=\int_{V_p}\frac{1}{2}\,[E]^t[D]^t\,dV_p \qquad (4)$$

where, [ξ] is the vector of mechanical displacements, [S] is the vector of mechanical strain components, [σ] is the vector of mechanical stress components, [D] is the vector of electrical displacement components, [E] is vector of electrical field components, ρ is the mass density, V_p is the volume of piezoelectric material and t represents transpose of the matrix.

If a set of discrete mechanical forces [f] is applied at locations (x_i, y_i) and a set of discrete electric charge output [q] is extracted at locations (x_i, y_i), then variation of mechanically applied and electrically extracted work may be written as

$$\delta W=\sum_{i=1}^{nf}[\xi]_{(xi,yi,t)}[f]_{(xi,yi,t)}+\\ +\sum_{j=1}^{nq}\delta\varphi_{(xi,yi,t)}q_{(xi,yi,t)}, \qquad (5)$$

where *nf* is the number of discrete mechanical forces, φ_i is the scalar electrical potential, *nq* is the number of discrete electrode pairs.

The linear electrostatic constitutive equation for piezoelectric material is given by [14]

$$\begin{Bmatrix}[\sigma]\\ [D]\end{Bmatrix}=\begin{bmatrix}[c_p^E] & -[e]^t\\ [e] & [\varepsilon^S]\end{bmatrix}\begin{Bmatrix}S\\ E\end{Bmatrix}, \qquad (6)$$

where, [c] is the elastic stiffness matrix, [e] is the matrix of piezoelectric constants, [ε] is the matrix of permittivity components.

Superscript E and S denote that the parameters are measured at constant electric field and constant strain respectively. Putting Eq. (6) in Eq. (1), the generalized Hamilton's principle for piezoelectric cantilever beam can be given as

$$\int_{t_1}^{t_2}[\int_{V_p}\rho_p\delta[\dot{\xi}]^t[\dot{\xi}]dV_p-\int_{V_p}\delta[S]^t[c^E][S]dV_p+\\ \int_{V_p}\delta[S]^t[e]^t[E]dV_p+\int_{V_p}\delta[E]^t[e][S]dV_p+\\ \int_{V_p}\delta[E]^t[\varepsilon^S][E]dV_p+\sum_{i=1}^{nf}\delta[\xi]_{(xi,yi,t)}[f]_{(xi,yi,t)}+\\ \sum_{j=1}^{nq}\delta\varphi_{(xi,yi,t)}q_{(xi,yi,t)}]dt=0 \qquad (7)$$

3. Piezoelectric Electromechanical Model for 31 Effects

A four node rectangular element with degree of freedoms per node as *u*, *v*, *w* in *x, y* and *z* directions is used to model the cantilever beam. Based upon Euler- Bernoulli's beam theory, the displacements are

considered on O*xz* plane only as shown in Fig. 1. The displacement field is then given by

$$\begin{Bmatrix} u \\ v \\ w \end{Bmatrix} = \begin{Bmatrix} -z\frac{\partial w}{\partial x} \\ 0 \\ w \end{Bmatrix}, \quad (8)$$

where, the displacement components u, v and w at thickness level z from the reference (neutral) surface are given in terms of the transverse deflection (w) of the reference surface. Hence the rectangular element is having 12 structural degree of freedom. It is assumed that each finite element of piezoelectric layer is completely covered with perfectly conductive electrodes on the top and bottom surface and therefore are electrical degree of freedom (voltage V_p across the electrode) is sufficient for modeling the electrical response of the element taken. Thus the rectangular element has 13 degree of freedom in total.

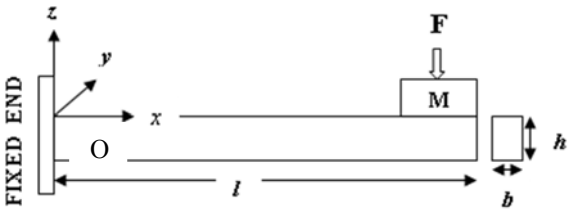


Fig. 1. A schematic rectangular cross-section piezoelectric bending sensor.

The mechanical strain components under the assumption of linear strain displacement can be given by

$$\{S\} = \begin{Bmatrix} S_x \\ S_y \\ 2S_{xy} \end{Bmatrix} = \begin{Bmatrix} \frac{\partial u}{\partial x} \\ \frac{\partial v}{\partial y} \\ \frac{\partial v}{\partial x} + \frac{\partial u}{\partial y} \end{Bmatrix} = -z \begin{Bmatrix} \frac{\partial^2 w}{\partial x^2} \\ \frac{\partial^2 w}{\partial y^2} \\ 2\frac{\partial^2 w}{\partial x \partial y} \end{Bmatrix} = -z \begin{Bmatrix} \frac{\partial^2 w}{\partial x^2} \\ 0 \\ 0 \end{Bmatrix} \quad (9)$$

The transverse displacement of any node k of the finite elements is assumed to vary in the polynomial form i.e.

$$w_k = [P]\{\mu\}, \quad (10)$$

where, [P] is the polynomial matrix, {μ} is the generalized coordinates.

The bending rotation about x axis cab be given as

$$\theta_{xk} = -\frac{\partial w}{\partial x_{(xk,yk)}} = -\frac{\partial [P]}{\partial x_{(xk,yk)}}\{\mu\} \quad (11)$$

The polynomial matrix is given as

$$[P] = [\,1\ x\ y\ x^2\ xy\ y^2\ x^3\ x^2y\ xy^2\ y^3\ x^3y\ xy^3\,]$$

$$\{\mu\} = [a_0\ a_1\ a_2\ a_3\ a_4\ a_5\ a_6\ a_7\ a_8\ a_9\ a_{10}\ a_{11}\ a_{12}]$$

Considering 4 nodes per element and 3 degree of freedom per nodes, one can defines 12 X 1 vector of nodal displacement as

$$\{\Psi\} = \{\, w_1\ \theta_{x1}\ \theta_{y1}\ w_2\ \theta_{x2}\ \theta_{y2}\ w_3\ \theta_{x3}\ \theta_{y3}\ w_4\ \theta_{x4}\ \theta_{y4}\,\}^t \quad (12)$$

This can be expressed as

$$\{\psi\} = [A]\{\mu\} \quad (13)$$

where [A] is the 12 × 12 transformation matrix whose elements are given by [P] and its derivatives through the definitions of w_k, and θ_{xk} is given in Eq.(10) and Eq.(11).

The transverse deflection as a function of nodal variable then can be given by

$$w_k = [N][\psi], \quad (14)$$

where

$$[N] = [P][A]^{-1} \quad (15)$$

The vector of transverse displacement and cross-section rotation is related to the vectors of nodal variable as

$$\begin{Bmatrix} \frac{\partial w}{\partial x} \\ 0 \\ w \end{Bmatrix} = [B_\eta][\psi]$$

Similarly the, the vector of curvature can be expressed as

$$\begin{Bmatrix} \frac{\partial^2 w}{\partial x^2} \\ 0 \\ 0 \end{Bmatrix} = [B_k][\psi]$$

Since piezoelectric material is poled in the thickness direction (z direction), the non- zero electric field component (which is assumed to be uniform in thickness direction) can be expressed as

$$E_Z = -\frac{\partial \varphi}{\partial z} = -\frac{v_p}{h_p}, \quad (16)$$

where the electric field potential is assumed to varying linearly across the electrodes i.e. the electric fields assumed to be uniform in z direction and h_p is piezoelectric material thickness. Then the electrode field vector can be written as

$$[E] = -[B_E]v_p\ , \quad (17)$$

where

$$B_E = \begin{Bmatrix} 0 \\ 0 \\ \frac{1}{h_p} \end{Bmatrix} \quad (18)$$

Based upon Hamilton's principle given by Eq.(7) the element matrix [m], stiffness matrix [k], electromechanical coupling matrix [θ], capacitance c_p and the mechanical forcing vector [f] can be expressed as

$$[m] = \int_{V_p}[B_\eta]^t[Z]^t\rho_p[Z]\left[B_\eta\right]dV_p \qquad (19.a)$$

$$[k] = \int_{V_p} Z^2[B_k]^t\left[c_p^E\right][B_k]dV_p \qquad (19.b)$$

$$[\theta] = \int_{V_p} Z[B_k]^t[e]^t dV_p \qquad (19.c)$$

$$c_p = \int_{V_p}[B_E]^t[\varepsilon^S][B_E]dV_p \qquad (19.d)$$

$$[f] = \int_S[N]^t f_w dS, \qquad (19.e)$$

where

$$[Z] = \begin{bmatrix} -z & 0 & 0 \\ 0 & -z & 0 \\ 0 & 0 & 1 \end{bmatrix}$$

As the width and thickness of piezoelectric cantilever is small as compared to length, therefore the stress components σ_2 and σ_3 may be neglected.

Hence the constitutive equation may be expressed as

$$\begin{bmatrix}[\sigma] \\ [D]\end{bmatrix} = \begin{Bmatrix}\sigma_1 \\ D_3\end{Bmatrix}\begin{bmatrix} c_{11}^E & -e_{31} \\ e_{31} & \varepsilon_{31}^S \end{bmatrix}\begin{Bmatrix} S_1 \\ E_3 \end{Bmatrix} \qquad (20)$$

The piezoelectric and dielectric component in Eq. (20) are given in contracted notations (i.e. Voigt's notation) where 1, 2 and 3 directions are coincident with x ,y and z directions.

The global equations of motion are then obtained by assembling the element matrices given by Eq. (19.a – 19.e) i.e.

$$[\boldsymbol{M}]\{\boldsymbol{\psi}\} + [\boldsymbol{C}]\{\boldsymbol{\psi}\} + [\boldsymbol{K}]\{\ddot{\boldsymbol{\psi}}\} - [\dot{\mho}]\{\boldsymbol{v}\} = [\boldsymbol{F}] \quad (21)$$

$$\left[\boldsymbol{c_p}\right]\{\boldsymbol{v}\} + [\boldsymbol{Q}] + [\mho]^t\{\boldsymbol{\psi}\} = \boldsymbol{0}, \qquad (22)$$

where, [M] is the global mass matrix, [K] is the global stiffness matrix, [℧] is the global electromechanical coupling matrix, [c_p] is the diagonal global capacitance matrix, $\{v\}$ is the global vector of voltage outputs, [Q] is the global vector of electric charge outputs, [C] is the global damping matrix.

4. Results and Discussion

The numerical characterization of piezoelectric cantilever with and without proof mass at free end for the two modes is presented for Eigen values and Eigen vectors. The effects of proof mass and length of beam on eigenfrequencies are obtained. Displacement and voltage generated are also investigated. Figs. 2 and 3 show the variation of eigenfrequencies of first two modes under different proof mass obtained by finite element method and compared with the published results. It is noted that the eigenfrequency of cantilever beam without proof mass is 123 Hz for the first mode and 684 Hz for the second mode respectively. These eigenfrequencies drops down continuously with increasing proof mass for first and second modes respectively. When the proof mass is 0.40 g at the free end of piezoelectric cantilever beam then eigenfrequencies changes from 123 Hz to 66 Hz for the first mode and 684 Hz to 474 Hz for the second mode respectively. Figs. 4 and 5 show the variation of tip displacement of piezoelectric cantilever beam for different lengths. It is observed that tip displacement for the first mode increases with increase in length of beam. For second mode the tip displacement first increases and then decreases with increase in length of beam as shown in Fig. 5. Therefore we anticipate that maximum voltage could be generated with second mode where displacement is maximum as compared to first mode. Figs. 6-9 show the harmonic response in terms of tip displacement and voltage generated of piezoelectric cantilever beam without proof mass under excitation force of 0.01 N at tip. The coefficient of damping assumed is 0.05. From Fig. 8 it observed that the maximum value of the tip displacement in second mode (684 Hz) at free end is 44 μm which was lower than that of first mode (i.e. 179 μm). However the voltage generated for second mode was 166 mV which was higher than that of first mode (130 mV) as shown in Figs.7 and 9. Figs. 10 and 11 show the variations of voltage generated by the piezoelectric cantilever beam for different proof mass. It is observed that voltage increased in the first mode with increasing proof mass. This is because of deflection of cantilever beam of first mode increased due to proof mass. In second mode, the voltage dropped down with increasing proof mass as shown in Fig. 11. Again, this is due to decreased deflection of cantilever beam due to proof mass.

5. Conclusions

A piezoelectric cantilever beam with different proof mass and different lengths has been modeled using finite element method and compared with the published results. It was noticed that the highest tip displacement of cantilever beam was reported in second mode at 25 mm length. It was further indicated that second mode of resonant frequency provided higher voltage as compared to first mode of cantilever beam without any proof mass. But when proof mass was added at free end the voltage dropped in the second mode and increased in first mode under a proof mass of 0.40 g.

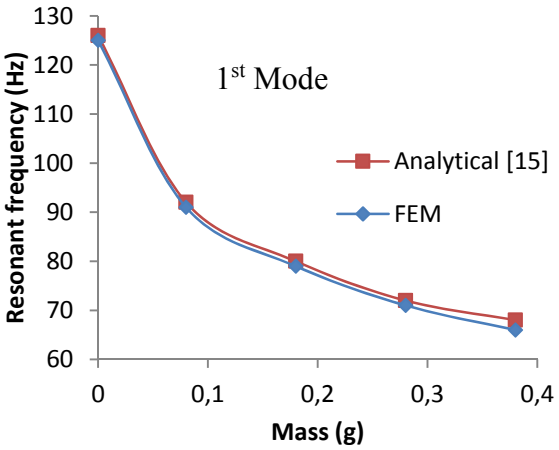


Fig. 2. Variation of eigenfrequency under different proof mass for the 1st mode.

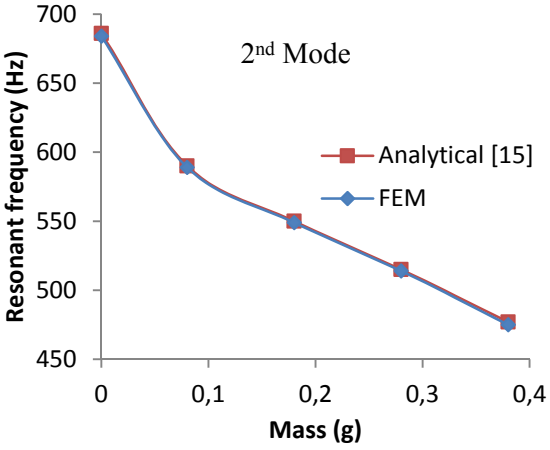


Fig. 3. Variation of eigenfrequency under different proof mass for the 2nd mode.

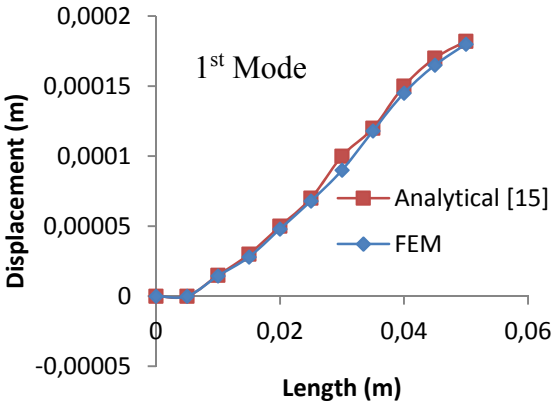


Fig. 4. Variation of tip displacement of piezoelectric cantilever beam for different lengths (1st mode).

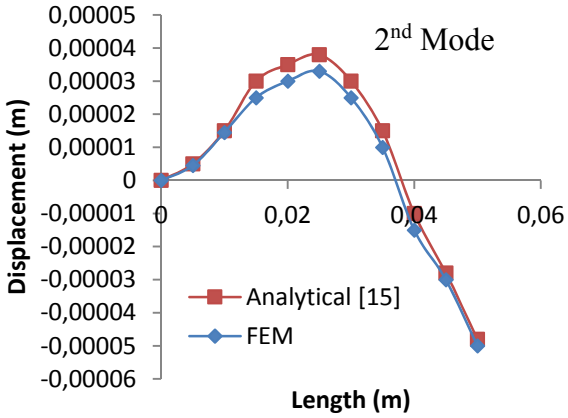


Fig. 5. Variation of tip displacement of piezoelectric cantilever beam for different lengths (2nd mode).

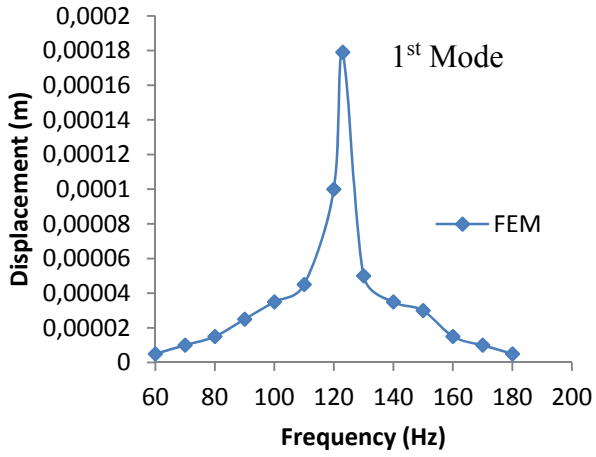


Fig. 6. Harmonic response in terms of tip displacement (1st mode).

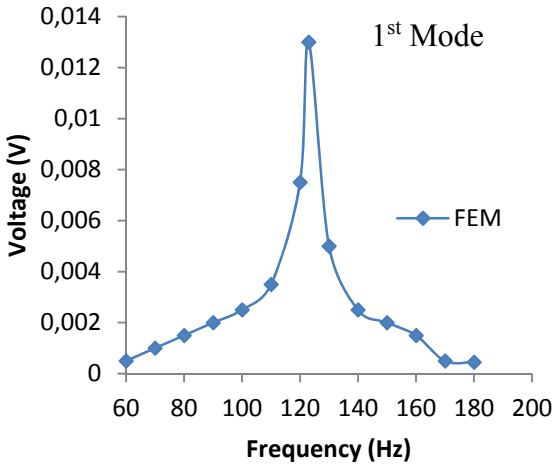


Fig. 7. Harmonic response in terms of voltage generated by piezoelectric cantilever beam (1st mode).

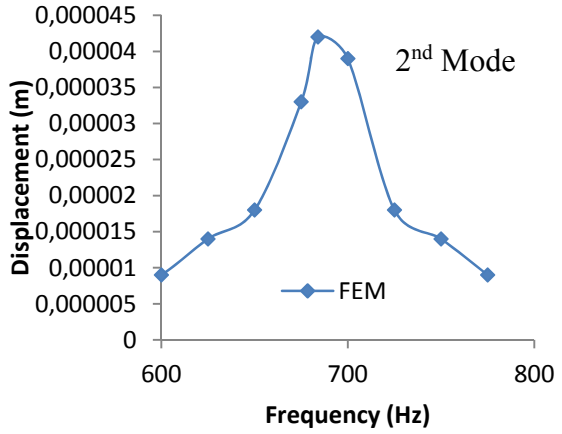


Fig. 8. Harmonic response in terms of tip displacement (2nd mode).

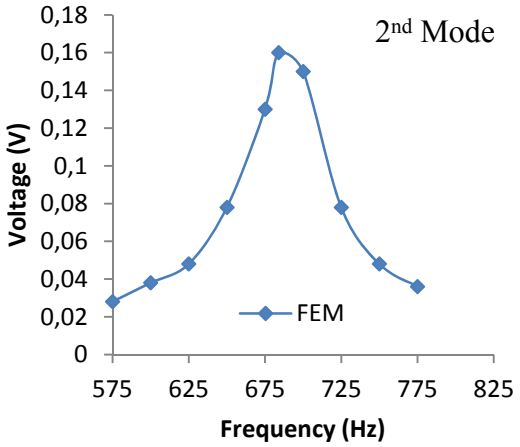


Fig. 9. Harmonic response in terms of voltage generated by piezoelectric cantilever beam (2nd mode).

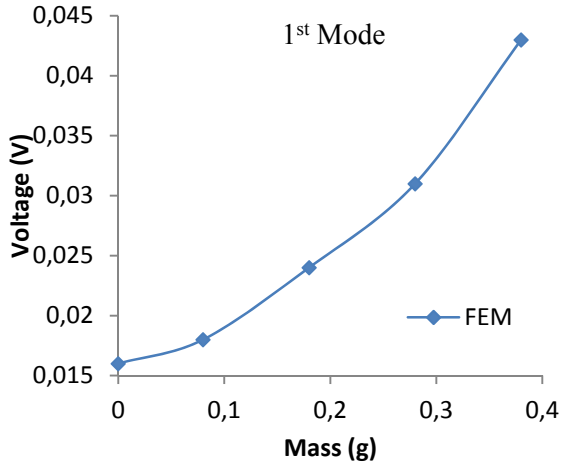


Fig. 10. Variations of voltage generated by the piezoelectric cantilever beam for different proof mass (1st mode).

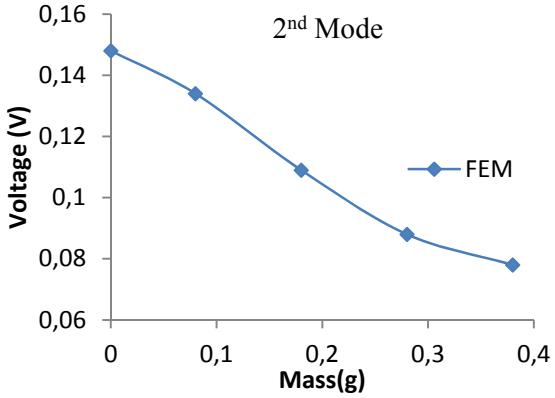


Fig. 11. Variations of voltage generated by the piezoelectric cantilever beam for different proof mass (2nd mode).

References

[1]. S. Tliba, H. Abou-Kandil, C. Prieur, Active vibration damping of a smart flexible structure using piezoelectric transducers: infinity design and experimental results, in *Proceedings of the 16th IFAC World Congress*, Vol. 16, Prague, Czech Republic, July 4–8, 2005.

[2]. B. Bandyopadhyay, T. C. Manjunath, M. Umapathy, Modeling, Control and Implementation of Smart Structures, LNCIS, *Springer*, 2007.

[3]. Huicong Liu, Chenggen Quan, Cho Jui Tay, Takeshi Kobayashi, and Chengkuo Lee, A MEMS-based piezoelectric cantilever patterned with PZT thin film array for harvesting energy from low frequency vibrations, in *International Conference on Optics in Precision Engineering and Nanotechnology, Physics Procedia,* 19, 2011, pp. 129–133.

[4]. Johnson T. J., Charnegie D., Clark W. W., Buric M., Kusic G., Energy harvesting from mechanical vibrations using piezoelectric cantilever beams, *Smart Structures and Materials: Damping and Isolation*, Vol. 6169, 2006, p. D1690, art. No. 61690D.

[5]. Ng T. H., Liao W. H., Feasibility study of a self-powered piezoelectric sensor, *Smart Structures and Materials: Smart Electronics, MEMS Bio-mems and Nanotechnology*, Vol. 5389, 2004, pp. 377–388.

[6]. Ng T. H., Liao W. H., Sensitivity analysis and energy harvesting for a self-powered piezoelectric sensor, *J. Intell. Mater. Syst. Struct.,* 2005, 16, pp. 785–797.

[7]. Jiang S. N., Li X. F., Guo S. H., Hu Y. T., Yang J. S., Jiang Q., Performance of a piezoelectric bimorph for scavenging vibration energy, *Smart Materials Structures*, 2005, 14, pp. 769–74.

[8]. Anderson T. A., Sexton D. W., A vibration energy harvesting sensor platform for increased industrial efficiency, in *Proceedings of the SPIE, Smart Structures and Materials: Sensors and Smart Structures Technologies for Civil, Mechanical, and Aerospace Systems*, 6174, 2006, pp. 621–629.

[9]. Mateu L., Moll F., Optimum piezoelectric bending beam structures for energy harvesting using shoe

inserts, *J. Intell. Mater. Syst. Struct.*, 2005, 16, pp. 835–45.

[10]. Roundy S., Leland E. S., Baker J., Carleton E., Reilly E., Lai E., et al., Improving power output for vibration-based energy scavengers, *IEEE Pervasive Comput*., 2005, 4, pp. 28–36.

[11]. Baker J., Roundy S., Wright P., Alternative geometries for increasing power density in vibration energy scavenging for wireless sensor networks, in *Proceeding of the 3rd International Energy Conversion Engineering Conference,* San Francisco, California, August 15–18, 2005.

[12]. Kim H. W., Batra A., Priya S., Uchino K., Markley D., Newnham R. E., et al., Energy harvesting using a piezoelectric cymbal, transducer in dynamic environment, *Jpn. J. Appl. Phys. 1, Regul Pap Short Notes Rev Pap*, 2004, 43, pp. 6178–83.

[13]. Carlos De Marqui Junior, Alper Erturk, Daniel J. Inman, An electromechanical finite element model for piezoelectric energy harvester plates, *Journal of Sound and Vibration,* 327, 2009, pp. 9-25.

[14]. IEEE Standard on Piezoelectricity, *IEEE Group on Sonics and Ultrasonics,* New York, 1978.

[15]. R. Ly, M. Rguiti, S. D'Astorg, A. Hajjaji, C. Courtois, A. Leriche, Modeling and characterization of piezoelectric cantilever bending sensor for energy harvesting, *Sensors and Actuators A: Physical,* Vol. 168, Issue 1, July 2011, pp. 95-100.

[16]. Atul, Vinayak Ranjan, Design and analysis of piezoelectric cantilever beam with PZT thin films array for vibration energy harvesting, in *Proceedings of the ISSS National Conference on MEMS, Smart Materials, Structures and Systems,* Pune, September 06-07, 2013.

2014 Copyright ©, International Frequency Sensor Association (IFSA) Publishing, S. L. All rights reserved. (http://www.sensorsportal.com)